POLITECNICO DI TORINO
Repository ISTITUZIONALE

SNO-Based Design of Wide-Angle Beam-Scanning Reflectarrays

Original
SNO-Based Design of Wide-Angle Beam-Scanning Reflectarrays / Beccaria, M., Niccolai, A., Massaccesi, A., Zich, R.E., Pirinoli, P.. - In: RADIO SCIENCE LETTERS. - ISSN 2736-2760. - ELETTRONICO. - 2:(2020), pp. 1-5. [10.46620/20-0047]

Availability:
This version is available at: 11583/2866692 since: 2021-02-15T17:42:22Z

Publisher:
URSI Publication

Published
DOI:10.46620/20-0047

Terms of use:

This article is made available under terms and conditions as specified in the corresponding bibliographic description in the repository

Publisher copyright

(Article begins on next page)

11 October 2026

SNO-Based Design of Wide-Angle Beam-Scanning Reflectarrays

M. Beccaria, A. Niccolai, A. Massaccesi, R. E. Zich, and P. Pirinoli

Abstract – In this article, the design of a passive reflectarray with beam-scanning capabilities over a wide scan range is addressed. The proposed approach is based on the use of an efficient evolutionary algorithm, Social Network Optimization, and on the definition of a proper optimization environment that allows the simultaneous optimization of the antenna radiation pattern for different pointing directions, keeping under control the computational cost of the procedure. The effectiveness of the method is validated through the experimental characterization of a prototype, whose performance is also compared with that of a conventional bifocal configuration.

1. Introduction

Nowadays, many applications require the use of a beam-scanning antenna; among the possible solutions for their realization, reflectarrays (RAs) have been considered in view of their interesting features when adopted to design fixed-beam antennas [1, 2].

The most straightforward way to obtain a beam-scanning RA is to introduce active elements, such as varactors, PIN diodes, or MEMS [3–6]: the resulting antenna performance is good, but its complexity significantly increases. An alternative is to use a passive reflectarray and steer the beam direction by either moving the feed along a circular arc to keep constant the distance with the RA surface or using a feed array [7–11]: the absence of active elements reduces the RA design's complexity, but at the cost of a degradation of the antenna radiation patterns, characterized by enlargement of the main beam, an increase in the side-lobe level (SLL), and a decrease in the maximum gain.

To overcome this problem, different techniques have been proposed, as that of designing a "bifocal" reflectarray [11], whose performance can eventually be enhanced using a double reflector configuration [12], or the use of the Phase Matching Method (PMM) [8]. An alternative solution consists in exploiting global evolutionary algorithms (EAs), even if their application to the optimization of an RA is still challenging for a number of reasons: the number of variables involved in the process is generally great, since they correspond to the degrees of freedom of the RA unit cells multiplied by the number of cells; the mathematical function that models the problem is computationally expensive or not accurate enough, and therefore there is a risk that the stochastic nature of the method provides a solution that behaves in a completely different way from the one predicted by the optimizer. Despite these drawbacks, some results on the use of the most popular EAs—such as Genetic Algorithm (GA), Particle Swarm Optimization (PSO), and differential evolution (DE)—for the optimization of shaped-beam, not uniformly spaced or multi-beam reflectarrays have been presented [13–17].

In this article, a more recent algorithm—Social Network Optimization (SNO)—which showed very good performance when used for the design of flat- [18] or shaped-beam [19] reflectarrays is applied to the design of a wide-angle, beam-scanning RA, covering a scan range from –40° to +40°. Particular care is devoted to the definition of the optimization environment, designed to guarantee accurate and reliable results and to minimize the process's numerical cost. Some very preliminary results were already presented [20, 21], where the performance of SNO and especially its convergence capability, was compared with that of another family of efficient EAs, the M_mC_n-BBO [22], an enhanced version of biogeography-based optimization (BBO) [23]. Here, the effectiveness of SNO is assessed by experimental characterization of a prototype, designed using the optimization algorithm, and comparison of its performance with that of an equivalent bifocal RA.

The main features of SNO are summarized in the next section. In Section 3 the considered problem and the related optimization environment are described. Finally, in Section 4 the performance of the optimized reflectarray is discussed and compared with that of the bifocal solution.

2. Social Network Optimization

SNO is a population-based algorithm that mimics the information-sharing process of online social networks. The population of the algorithm consists of the users of the considered social network that share their ideas and interact online. Each user is characterized by its opinion, which is shared by means of a post (in the metaphor, the candidate solution of the optimization problem). The post is evaluated by the social network and receives a visibility value (the cost value of the problem) that indicates how probable it is that another user can read it and be influenced by it.

The online interaction takes place through two different networks: the friend network, characterized by

Manuscript received 29 August 2020.

M. Beccaria, A. Massaccesi, and P. Pirinoli are with the Department of Electronics and Telecommunications, Politecnico di Torino, Corso Duca degli Abruzzi 24, 10129 Torino, Italy; e-mail: michele.beccaria@polito.it, andrea.massaccesi@polito.it, paola.pirinoli@polito.it.

A. Niccolai and R. E. Zich are with the Department of Energy, Politecnico di Milano, Via La Masa 34, 20156 Milano, Italy; e-mail: alessandro.niccolai@polimi.it, riccardo.zich@polimi.it.

Table 1. Comparison between genetic algorithm (GA), particle swarm optimization (PO), and SNO.

Function	GA	PSO	SNO
Ackley	2.4	3	**0.99**
Griewank	1.63	1.27	**1.17**
Penalty 1	0.56	5.32	**0.19**
Rastrigin	71.59	143.11	**8.91**
Rosenbrock	23.17	**19.36**	40.96
Schwefel-221	**4.52**	13.29	10.36
Sinc-N	0.73	1	**0.09**
Sphere	0.18	0.07	**0.05**

strong connections among users and a slow evolution rate, and the trust network, characterized by weaker interactions and an evolution based on posts' visibility value. Each user exchanges opinions with other individuals, being influenced by both networks. The interaction is based on the following equation:

$$\mathbf{o}(t+1) = \mathbf{o}(t) + \alpha[\mathbf{o}(t) - \mathbf{o}(t-1)] + \beta[\mathbf{a}(t) - \mathbf{o}(t)] \tag{1}$$

where $\mathbf{o}$ is the user opinion and $\mathbf{a}$ is the attracting idea, obtained by means of a single-point crossover from the ideas deriving from the two networks.

SNO has been compared with GA and PSO, through application to several benchmark functions that are widely used for EA testing, since each of them has unique features useful in measuring algorithm performance in different scenarios. More details on these functions and their complete mathematical formulation can be found in [24]. Table 1 reports the average cost value obtained by application of the three algorithms to the listed benchmark functions after 5,000 objective function calls and considering 50 independent trials. In most cases (the bolded values are the best results for each function), SNO outperforms the other two algorithms, and this confirms its good features.

3. The Optimization Environment

The optimization problem addresses the design of an RA with $N \times N$ unit cells, showing scanning capabilities over the range $\left[\theta^s_{\min}, \theta^s_{\max}\right]$ in the elevation plane. The problem is intrinsically multiobjective, but to keep the computational cost under control while still guaranteeing good convergence and reliability, a proper cost function was introduced that is the linear combination of different terms, each representing a specific objective:

$$C(\mathbf{d}, S_i) = \sum_{i \in S} \lambda_i \cdot (c_1(\mathbf{d}, S_i) + c_2(\mathbf{d}, S_i)) \tag{2}$$

In (2), $\mathbf{d}$ is the vector of variables used to control the optimization process, λ_i are scalar coefficients, and S is the set of directions of maximum radiation considered, during the optimization, within the scan coverage.

The c_1 function is defined as the integral of the error Δ_{S_i} between the radiation pattern evaluated with the aperture field method [1] and the values of the optimization variables provided by SNO and a predefined 3D mask:

$$c_1(\mathbf{d}, S_i) = \iint \Delta_{S_i}(\theta, \phi) d\theta d\phi \tag{3}$$

The function c_2 represents the scan-angle error $\Delta\theta_{S_i}$—i.e., the squared value of the difference between the desired direction of maximum radiation θ_s and the actual one, $\theta_{\max}$:

$$c_2(\mathbf{d}, S_i) = \Delta\theta_{S_i} = \left[(\theta_{S_i} - \theta_{\max}) \frac{180}{\pi}\right]^2 \tag{4}$$

It was introduced to speedup the algorithm's convergence and guarantee that the direction of maximum radiation is properly found.

The variables collected in the vector $\mathbf{d}$ are of two types: free geometrical parameters characterizing each unit cell and the Beam Deviation Factor (BDF), defined as the ratio between $\theta_{\max}$ and the angle of incidence θ_{inc} between the impinging field and the direction orthogonal to the RA surface. A BDF is associated to each considered direction of maximum radiation. Since they have different domains of definition, variables normalized in the range [0; 1] are used.

To improve the effectiveness of SNO and guide it to find a feasible solution, the available information about the physics of the considered problem is implemented in the optimization environment. In particular, the masks corresponding to the different pointing directions are not equal, to take into account the fact that the beam steering affects the radiation patterns, with a widening of the main beam and an increase of the SLL. Moreover, symmetrical scan coverage can be obtained with a symmetrical distribution of the unit cells: this means that only half of the scanning range can be considered during the optimization, and also that the symmetries can be used to reduce the size of the problem and consequently the computational time for solving it.

4. Results

In the considered example, $N = 24$ and each unit cell has a size equal to $\lambda/2$, at $f_0 = 30$ GHz, for a total size of the square RA aperture of $12\lambda \times 12\lambda$. The radiating elements are square patches, printed on a Diclad 527 substrate with a thickness of 0.8 mm and $\varepsilon_r = 2.55$; the phase of the unit cell reflection coefficient is controlled through the patch side W [19]. The aperture is illuminated by a smooth wall horn whose radiation pattern can be modeled as $[\cos(\theta)]^q$, with $q = 12.5$ [25]. The focal distance from the phase center of the feed to the aperture is $f/D = 1.2$, to reduce the taper. A sketch of the resulting configuration is shown in Figure 1.

The RA's total number of degrees of freedom is equal to $N^2 = 576$, but, considering the symmetries in the patches distribution, it reduces to $N_{\text{DF}} = 144$. Moreover, only the positive half-scan range is considered in the optimization: as a consequence, $\theta^s_{\max}$ was

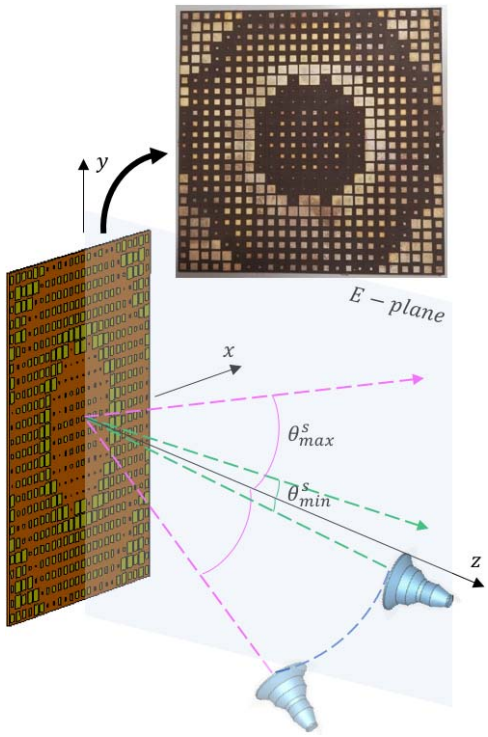

Figure 1. Sketch of the antenna configuration, with two positions of the feed corresponding to the directions of maximum radiation characterized by $\theta^s_{\min}$ and $\theta^s_{\max}$, and photo of prototype of the RA designed with SNO.

chosen equal to 40°, while $\theta^s_{\min} = 10^{\circ}$, to avoid radiation in the broadside direction that would be affected by the blockage introduced by the feed. In this interval, four directions of maximum radiation—i.e., $\theta_{\max} = 10°$, 20°, 30°, 40°—were considered in the optimization process; therefore, the total number of optimization variables is $N_{\mathrm{DF}} + 4\mathrm{BDF}$. The starting position of the feed is specular to the direction of maximum radiation of the RA identified by $\theta^s_{\min}$; the feed is then moved along a circular arc to cover the scanning range up to $\theta^s_{\max}$ (see Figure 1).

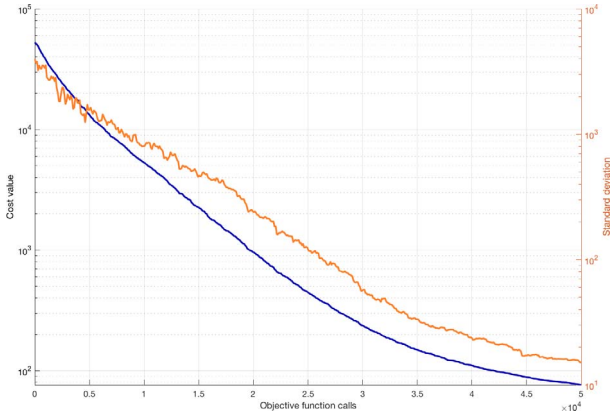

Figure 2. Average value of the curves of convergence (blue line) and corresponding standard deviation (orange line).

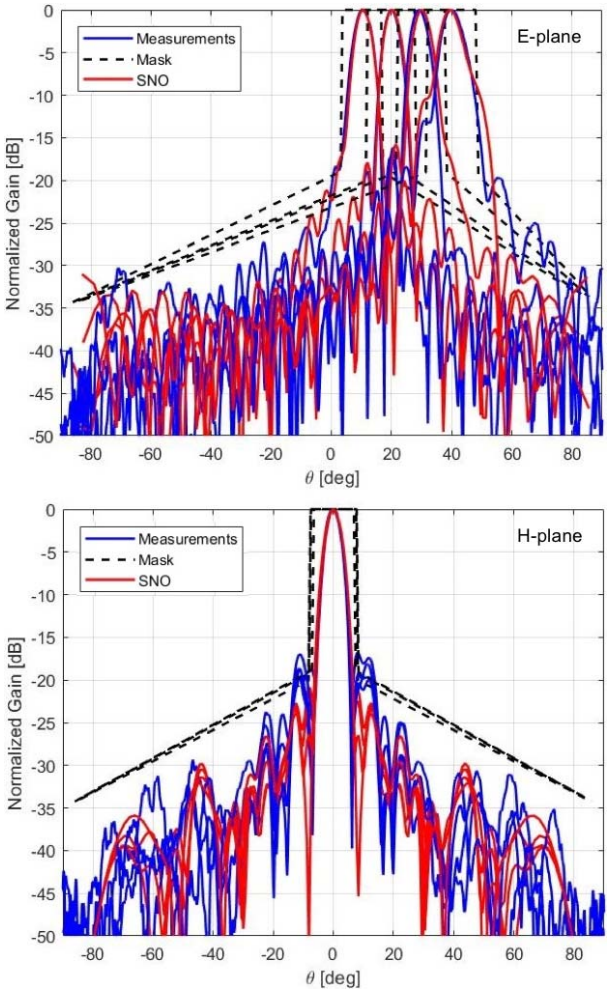

Figure 3. Optimized RA: normalized radiation patterns at the end of the optimization process and measured ones in the E-plane (top) and H-plane (bottom) for the pointing directions in the E-plane $\theta_{\max} = 10°$, 20°, 30°, 40°; masks adopted during the optimization process.

The termination criterion adopted for the optimization is 50,000 objective function calls. The average value of the curves of convergence and the corresponding standard deviation obtained considering 40 independent trials are plotted in Figure 2; they prove the good convergence capability of the process and also its reliability.

The radiation patterns obtained at the end of the process in the four considered directions of maximum radiation in the E- and H-planes are plotted in Figure 3, together with the adopted masks. In the same figure, the measured patterns relative to the prototype shown in the inset of Figure 1 are shown. Good agreement can be seen between the results obtained at the end of the optimization and the measured ones; above all, they satisfy the masks almost everywhere. This proves the effectiveness of the developed technique and the beam-scanning capability of the RA. Note that the radiation

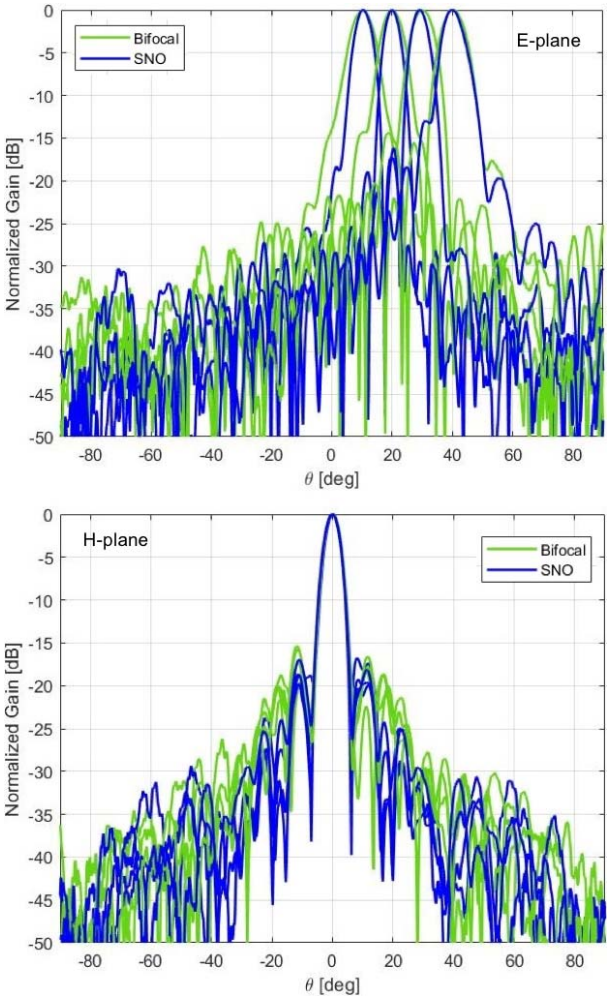

Figure 4. Measured normalized radiation patterns in the E-plane (top) and H-plane (bottom) for the pointing direction in the E-plane $\theta_{max} = 10°, 20°, 30°, 40°$: optimized RA (–); bifocal RA (–).

patterns for the negative part of the scan range are not shown, since they are symmetrical to the plotted ones.

To further validate the efficiency of the proposed method, the RA performance was compared with that of a bifocal configuration, with the same size, designed to compensate the average of the phase maps needed to have maximum radiation for $\theta_{max} = \pm 40°$. The measured radiation patterns in the two principal planes for the resulting configuration are plotted in Figure 4, together with those for the optimized RA. Also in this case, in the E-plane only the radiation patterns for positive scanning angles are shown. The quality of the optimization process is clear: the radiation patterns of the optimized configuration are characterized by narrower main beams and lower SLLs. Finally, in Figure 5, the variation of the gain with the scanning angle is reported, for both the optimized and the bifocal RAs. The continuous lines represent the evaluated gain, while the circles show the measured values. These results confirm that the optimized RA outperforms the

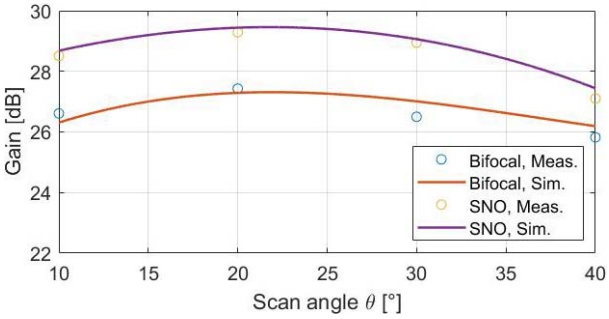

Figure 5. Variation of the evaluated and measured values of the gain, as a function of the scan angle for the optimized and bifocal RA.

bifocal one: the maximum gain that occurs for almost the same angle is 2 dB higher, at a cost of a slightly larger variation of the gain over the considered subrange, equal to $\Delta G = 2$ dB for the SNO solution and $\Delta G = 1.7$ dB for the bifocal one.

5. Conclusions

In this article, the design of a beam-scanning passive reflectarray antenna carried out with a promising evolutionary algorithm—Social Network Optimization—is presented, together with a description of the optimization environment developed to maximize the optimization efficiency and the accuracy and reliability of the obtained solution. Those features are proven through the experimental characterization of a prototype and the comparison of its performance with that of a bifocal RA.

6. Acknowledgment

The authors would like to thank Gianluca Dassano from the Politecnico di Torino for his valuable help in the experimental characterization of the antenna prototypes.

7. References

1. J. Huang and J. A. Encinar, *Reflectarray Antennas*, Hoboken, NJ, Wiley-IEEE Press, 2008.
2. P. Nayeri, F. Yang, and A. Z. Elsherbeni, *Reflectarray Antennas: Theory, Designs, and Applications*, Hoboken, NJ: Wiley-IEEE Press, 2018.
3. S. V. Hum, M. Okoniewski, and R. J. Davies, "Modeling and Design of Electronically Tunable Reflectarrays," *IEEE Transactions on Antennas and Propagation*, **55**, 8, August 2007, pp. 2200–2210.
4. M. Riel and J.-J. Laurin, "Design of an Electronically Beam Scanning Reflectarray Using Aperture-Coupled Elements," *IEEE Transactions on Antennas and Propagation*, **55**, 5, May 2007, pp. 1260–1266.
5. E. Carrasco, M. Barba, and J.A. Encinar, "X-Band Reflectarray Antenna With Switching-Beam Using PIN Diodes and Gathered Elements," *IEEE Transactions on Antennas and Propagation*, **60**, 12, December 2012, pp. 5700–5708.
6. O. Bayraktar, O. A. Civi, and T. Akin, "Beam Switching Reflectarray Monolithically Integrated With RF MEMS

Switches," *IEEE Transactions on Antennas and Propagation*, **60**, 2, February 2012, pp. 854–862.
7. P. Nayeri, F. Yang, and A. Z. Elsherbeni, "Beam-Scanning Reflectarray Antennas: A Technical Overview and State of the Art," *IEEE Antennas and Propagation Magazine*, **57**, 4, August 2015, pp. 32–47.
8. G.-B. Wu, S.-W. Qu, and S. Yang, "Wide-Angle Beam-Scanning Reflectarray With Mechanical Steering," *IEEE Transactions on Antennas and Propagation*, **66**, 1, January 2018, pp. 172–181.
9. X. Yang, S. Xu, F. Yang, M. Li, H. Fang, et al., "A Mechanically Reconfigurable Reflectarray With Slotted Patches of Tunable Height," *IEEE Antennas and Wireless Propagation Letters*, **17**, 4, April 2018, pp. 555–558.
10. P. Mei, S. Zhang, and G. F. Pedersen, "A Low-Cost, High-Efficiency and Full-Metal Reflectarray Antenna With Mechanically 2-D Beam-Steerable Capabilities for 5G Applications," *IEEE Transactions on Antennas and Propagation*, **68**, 10, October 2020, pp. 6997–7006.
11. P. Nayeri, F. Yang and A. Z. Elsherbeni, "Bifocal Design and Aperture Phase Optimizations of Reflectarray Antennas for Wide-Angle Beam Scanning Performance," *IEEE Transactions on Antennas and Propagation*, **61**, 9, September 2013, pp. 4588–4597.
12. E. Martinez-de-Rioja, J. A. Encinar, R. Florencio, and C. Tienda, "3-D Bifocal Design Method for Dual-Reflectarray Configurations With Application to Multibeam Satellite Antennas in Ka-Band," *IEEE Transactions on Antennas and Propagation*, **67**, 1, January 2019, pp. 450–460.
13. H. Yang, F. Yang, S. Xu, Y. Mao, M. Li, et al., "A 1-Bit 10×10 Reconfigurable Reflectarray Antenna: Design, Optimization, and Experiment," *IEEE Transactions on Antennas and Propagation*, **64**, 6, June 2016, pp. 2246–2254.
14. Y. Aoki, H. Deguchi, and M. Tsuji, "Reflectarray With Arbitrarily-Shaped Conductive Elements Optimized by Genetic Algorithm," 2011 IEEE International Symposium on Antennas and Propagation (APSURSI), Spokane, WA, USA, July 3–8, 2011, pp. 960–963.
15. D. Kurup, M. Himdi, and A. Rydberg, "Design of an Unequally Spaced Reflectarray," *IEEE Antennas and Wireless Propagation Letters*, **2**, December 2003, pp. 33–35.
16. P. Nayeri, F. Yang, and A. Z. Elsherbeni, "Design of Single-Feed Reflectarray Antennas With Asymmetric Multiple Beams using the Particle Swarm Optimization Method", *IEEE Transactions on Antennas and Propagation*, **61**, 9, September 2013, pp. 4598–4605.
17. C. Geaney, J. Sun, S. V. Hum, E. S. Rogers, E. Martinez-de-Rioja, et al., "Synthesis of a Multi-Beam Dual Reflectarray Antenna Using Genetic Algorithms," 2017 IEEE International Symposium on Antennas and Propagation & USNC/URSI National Radio Science Meeting, San Diego, CA, USA, July 9–14, 2017, pp. 1179–1180.
18. A. Niccolai, X. Pan, P. Pirinoli, F. Yang, R. E. Zich, et al., "Flat Beam Optimization of 1-Bit Reflectarray by Means of Social Network Optimization," 2018 IEEE International Symposium on Antennas and Propagation & USNC/URSI National Radio Science Meeting, Boston, MA, USA, July 8–13, 2018, pp. 543–544.
19. A. Niccolai, R. Zich, M. Beccaria, and P. Pirinoli, "SNO Based Optimization for Shaped Beam Reflectarray Antennas," 2019 13th European Conference on Antennas and Propagation (EuCAP), Krakow, Poland, March 31–April 5, 2019, pp. 1–4.
20. M. Beccaria, A. Massaccesi, P. Pirinoli, A. Niccolai, and R. Zich, "SNO and mBBO Optimization Methods for Beam Scanning Reflectarray Antennas," 2019 IEEE International Symposium on Antennas and Propagation and USNC-URSI Radio Science Meeting, Atlanta, GA, USA, July 7–12, 2019, pp. 1037–1038.
21. A. Niccolai, M. Beccaria, A. Massaccesi, R. E. Zich, and P. Pirinoli, "Optimization of Beam Scanning Reflectarray using M_QC_{10}-BBO and SNO Algorithms," 2019 International Conference on Electromagnetics in Advanced Applications (ICEAA), Granada, Spain, September 9–13, 2019, pp. 0506–0509.
22. P. Pirinoli, A. Massaccesi, and M. Beccaria, "Application of the M_mC_n-BBO Algorithms to the Optimization of Antenna Problems," 2017 International Conference on Electromagnetics in Advanced Applications (ICEAA), Verona, Italy, September 11–15, 2017, pp. 1850–1854.
23. D. Simon, "Biogeography-Based Optimization," *IEEE Transactions on Evolutionary Computation*, **12**, 6, December 2008, pp. 702–713.
24. D. Simon, *Evolutionary Optimization Algorithms*, Hoboken, NJ, John Wiley & Sons, 2013.
25. M. Beccaria, G. Addamo, P. Pirinoli, M. Orefice, O. Peverini, et al., "Feed System Optimization for Convex Conformal Reflectarray Antennas," 2017 IEEE International Symposium on Antennas and Propagation & USNC/URSI National Radio Science Meeting, San Diego, CA, USA, July 9–14, 2017, pp. 1187–1188.